Int. J. Electrochem. Sci., 8 **(2013)** 8058 - 8076

International Journal of
ELECTROCHEMICAL
SCIENCE
www.electrochemsci.org

New Insight into Vinylethylene Carbonate as a Film Forming Additive to Ethylene Carbonate-Based Electrolytes for Lithium-Ion Batteries

Shou-Dong Xu[1,2], *Quan-Chao Zhuang*[1,*], *Jing Wang*[1], *Ya-Qian Xu*[1], *Ya-Bo Zhu*[1,2]

[1] Lithium-ion Batteries Laboratory, School of Materials Science and Engineering, China University of Mining and Technology, No.8, South 3rd Ring Road, Quanshan District, Jiangsu, Xuzhou 221116, China
[2] School of Chemical Engineering and Technology, China University of Mining and Technology, No.8, South 3rd Ring Road, Quanshan District, Jiangsu, Xuzhou 221116, China
[*]E-mail: zhuangquanchao@126.com

Received: 3 April 2013 / *Accepted:* 16 April 2013 / *Published:* 1 June 2013

The effects of vinylethylene carbonate (VEC) as electrolyte additive and the content of VEC in ethylene carbonate (EC)-based electrolyte on the formation mechanisms of solid electrolyte interphase (SEI) film and the electrochemical properties of the graphite electrodes in lithium-ion batteries are investigated by cyclic voltammetry (CV) measurement and charge-discharge test. Enhanced electrochemical performance is observed for graphite electrodes in VEC-containing electrolytes with low content. Scanning electron microscopy (SEM) and Fourier transform infrared (FTIR) spectroscopy are used to investigate the morphology and the surface chemistry of graphite electrodes cycled in VEC-free and VEC-containing electrolytes. Finally, electrochemical impedance spectroscopy (EIS) is used in order to better understand the formation mechanisms of SEI film in VEC-containing electrolyte. The results reveal that the main reduction products of the SEI film formed in VEC-containing electrolyte are VEC polymerizes, Li_2CO_3 and $ROCO_2Li$. The SEI film covering graphite electrodes in VEC-containing electrolyte can be more stable during lithium ions insertion, and be flexible to accommodate the volume changes of graphite material, resulting in a better reversibility of lithium ions insertion and extraction.

Keywords: lithium-ion battery; graphite electrode; solid electrolyte interface film; vinylethylene carbonate; additives

1. INTRODUCTION

Lithium-ion batteries have been widely used for portable electronics and more recently are finding usage in transportation applications, because of their high energy density, slow self-discharge,

lack of memory effect and long cycle life [1,2]. Currently, graphite is the most widely adopted anode material in commercial lithium-ion batteries due to its high capacity (372 mAh g^{-1}) and low potential. It is generally known that during the first intercalation of lithium into the graphite electrode, the compositions of electrolyte solution are reduced to form a surface film on graphite electrode that is generally called the solid electrolyte interphase (SEI) [3-5]. The formation of the SEI leads to an irreversible loss of capacity on the initial charge-discharge cycles of the lithium-ion batteries. However, the SEI film suppresses, if the film forming process is optimized, any further electrolyte decomposition and avoids the exfoliation of the graphite structure [6]. At the same time, it allows the passage of lithium ions. Thus, the formation of an efficient SEI film is therefore the key for the achievement of a good reversibility of the battery even for prolonged cycling.

In the past decades, there have been numerous investigations on improving the properties of SEI film in order to improve the battery performance and this field is an ongoing topic of research [7-11]. Generally, the properties of the SEI film formed on graphite are multiple depending strongly on the electrolyte composition and the nature of impurities. Therefore, the use of film forming additives that predominantly react on the graphite surfaces to form SEI film of improved properties, suppression of solution reactions (less irreversible capacity), and efficient passivation is one of the most efficient methods to improve lithium-ion battery performances. Up to mow, many film forming additives such as SO_2 [12], Li_2CO_3 [13-15], K_2CO_3 [16,17], lithium bis (oxalato) borate (LiBOB) [18], ethylene sulfite [19], propylene sulfite (PS) [20], vinyl ethylene sulfite (VES) [21], prop-1-ene-1,3-sultone (PES) [22], vinylene trithiocarbonate (VTC) [23], fluoroethylene Carbonate (FEC) [24-27] and vinylene carbonate (VC) [23,28-30] were successfully employed to improve the electrochemical performance and to modify the surface chemistry of graphite or Si anodes for lithium-ion batteries. Among these additives, VC is regarded as the most widely used SEI forming improver additive. Although VC has been extensively used to improve the electrochemical performance and thermal stability of lithium ion batteries [31], some efforts have been focused to design other effective SEI forming improver additive due to its unstable structure [32].

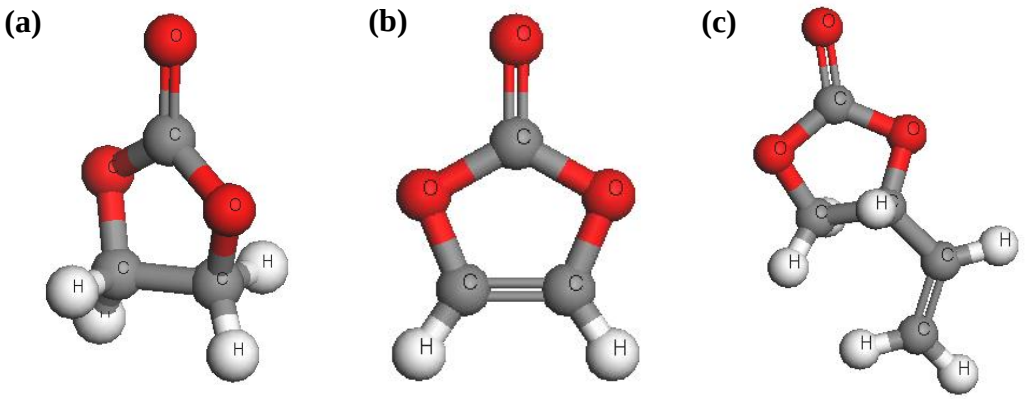

Figure 1. The molecular structure of (a) EC, (b) VC and (c) VEC.

Vinylethylene carbonate (VEC) has a similar structure to VC, also has the ring molecule structural and carbon double bonds, as seen in Fig. 1. It is supposed that VEC should have a stable structure because the double bond of VEC is somewhat electron rich thus not very reactive towards double bonds. Hu et al. [33,34] studied VEC as an additive in propylene carbonate (PC)-based electrolyte, they found that VEC could improve the cell performance due to the stable SEI film resulting from the reductive decomposition of VEC on the graphite surface. Nam et al. [35] reported that the electrochemical behavior and thermal properties of VEC with triphenyl phosphate-based electrolyte, the discharge capacity, rate capability, coulombic efficiency and cycleability were all improved when the cells contained 1wt% VEC in electrolyte. Fu et al. [36] investigated the electrochemical performance of natural graphite in 1-ethyl-3-methylimidazolium (EMI)-bis(trifluoromethyl-sulfonyl) imide (TFSI)-LiTFSI ionic liquid electrolyte with 5 wt% ethylene carbonate (EC) and 5 wt% VEC, and they considered the improvement on electrochemical performance in their study was mainly attributed to the cooperation of EC and VEC, because the SEI formation of EC/VEC is a continuous process in the potential range from 1.45 V till lithium ion inserting into graphite structure.

As discussed above, VEC has been validated to be an efficient film forming additive for the PC-based electrolytes and was capable of preventing PC cointercalation into graphite flakes [33,34]. However, the commercial electrolytes commonly use EC in most cases as the main solvent, as to our best knowledge, few papers discussed the effect of VEC as electrolyte additive in EC-based electrolyte on the formation mechanisms of the SEI film covering graphite electrodes for lithium-ion batteries. Furthermore, although VEC has been widely used as a film formation additive in commercial electrolyte, the content of VEC adding in EC-based electrolyte is often operating by experience, and the effect of the content of VEC on the surface film formation and the electrochemical properties is still not clear, that is to say, there is lack of a clear understanding that whether the more VEC additive in EC-based electrolyte should take the better electrochemical properties of graphite electrodes and how much amount of VEC is appropriate for the electrolyte.

Hence, the aim of this paper is to investigate the effect of VEC as electrolyte additive in the electrolyte of 1M $LiPF_6$ dissolved in EC/diethy carbonate (DEC)/dimethyl carbonate (DMC) (1:1:1, v/v/v) on SEI film formation covering graphite electrode and the content of VEC additive in the electrolyte on the electrochemical properties of graphite electrodes, and to better understand the formation mechanisms of SEI film. Charge-discharge tests and cyclic voltammograms (CV) were introduced to research the electrochemical behaviors; the morphology and surface chemistry of graphite electrodes were investigated by scanning electron microscopy (SEM) combining with Fourier transform infrared spectroscopy (FIIR) techniques. To elaborate the possible mechanisms of the enhanced performances of graphite electrode in the VEC-containing electrolyte, electrochemical impedance spectroscopy (EIS) measurement was applied; the obtained data were fitted using Zview software, and variations of kinetics parameters with electrode polarization potential.

2. EXPERIMENTAL

2.1 Theoretical calculations

The calculations of the frontier molecular orbital energy of the solvents and additives in this study were performed using Materials Studio software based on the density functional theory (DFT) with $DMol^3$ module. The geometry optimizations of the organic carbonates were carried out with Broyden-Fletcher-Goldfarb-Shanno (BFGS) method with GGA-BLYP basis set.

2.2 Preparation of the graphite electrode

The graphite electrode used in this study was prepared by spreading a mixture comprising, by weight, 90 % mesophase-pitch-based carbon fibers (MCF, Petoca, Japan) and 10 % PVdF (HSV910, USA) binder dissolved in N-methyl-2-pyrrolidone (NMP, Alfa Aaesar, A. Johnson Matthey Company, China) onto a copper foil current collector.

2.3 Electrochemical measurement

CV and EIS were carried out by a laboratory-made three-electrode glass cell with Li foils as the counter and reference electrode using an electrochemical workstation (CHI660C, Chenhua Co., Shanghai, China) at room temperature. The area of the work electrode is 1.5×1.5 cm^2. Charge-discharge test was evaluated using CR2032-type coin cell. Coin cell was assembled with a graphite working electrode and a Li foil counter electrode, separated by a polypropylene microporous separator (Celgard 2400) soaked in electrolyte. The electrolyte was 1M $LiPF_6$ dissolved in EC/ DEC/ DMC (1:1:1, v/v/v, Shanshan Inc., China). VEC (Shanshan Inc., China) as an electrolyte additive was added at different volume ratio (0.5, 1.0, 3.0, 5.0 and 10.0 %) with the above electrolyte.

CV was measured at a scan rate of 1 mV s^{-1} in the potential range of 3.0-0.0 V (*vs*. Li/Li^+). EIS was measured over the frequency range from 10^5 to 10^{-2} Hz with a potentiostatic signal amplitude of 5 mV. The electrode was equilibrated for 1 h before the EIS measurements, in order to attain steady-state conditions. The coin cells were galvanostatically charged and discharged in a battery analzyers (Neware, Shenzhen, China) over a range of 1.5-0.001 V *vs*. Li/Li^+ at a constant current density of 0.1C (1C=372 mA g^{-1}).

2.4 SEM and FTIR measurements

The specimen after CV test was transferred into the glove box and scraped from the copper foil current collector, washed in DMC and dried under vacuum to remove the residual electrolyte. The change in morphology of the graphite electrode before and after electrochemical tests in different electrolyte compositions was investigated by a LEO 1530 Field Emission Scanning Electron Microscopy (FE-SEM, Oxford Instrument). The components of the surface film formed on cycled

electrodes were characterized by FTIR (Tensor-27, BRUKER) using a pellet containing a mixture of KBr in the range of 4000~650 cm^{-1}.

3. RESULTS AND DISUSSION

3.1 DFT calculations

Table 1. The calculation results of the frontier orbital energy of solvents and additives.

		HOMO (ev)	LUMO (ev)	ΔE_g^a (ev) ΔE_g^a = LUMO-HOMO
solvent	EC	-6.883	-0.389	6.494
	DEC	-6.417	0.007	6.410
	DMC	-6.584	-0.144	6.440
additive	VEC	-6.786	-1.555	5.231
	VC	-6.187	-1.121	5.066

Table 1 shows the frontier molecular orbital energy of the solvents used in this study and the additives of VC and VEC. Based upon molecular orbital theory, a molecule with a higher energy lever of highest occupied molecular orbital (HOMO) should be easier to donate electrons. That is to say, the oxidation potential of the organic molecule is low, and the antioxidation of the organic molecule is poor. On the other hand, a molecule with a lower energy level of lowest unoccupied molecular orbital (LUMO) should be a better electron acceptor and more reactive on the negatively charged surface of the electrode [21,37,38]. From Table 1, it can be seen that energy levels of LUMO of VC and VEC additives are lower than EC, DMC and DEC solvents, and VEC with the lowest energy levels of LUMO. In other words, VEC will be reduced prior to VC additive and EC, DMC and DEC solvents during the first lithium ion insertion process. Among the various carbonate solvents used in this study, the order of reactivity toward reduction is VEC > EC > DMC > DEC. It is clearly indicated that VEC molecules can easily accept electrons and bear a higher reaction activity. So adding VEC into the electrolyte can prevent the further reaction between the solvent and lithium ions.

3.2 CV Results

Figure 2 shows the cyclic voltammetry recorded on the graphite electrode in the electrolytes of 1 $mol \cdot L^{-1}$ $LiPF_6$ in EC: DEC: DMC and with different volume ratio (0.5, 1.0, 3.0, 5.0 and 10.0 %) of VEC additive. For VEC-free electrolyte, as seen in Fig. 2(a), there are two reductive current peaks (peak α and β) can be observed in the first lithium ion insertion process during the potential region from 1.0 to 0.5 V. After the first cycle, peaks α and β disappear, implying that peaks α and β are attributed to the formation of the SEI film on the surface of the graphite. According to our previous study [17,39] and Naji et al. [40,41], the reduction process of EC mainly includes two steps.

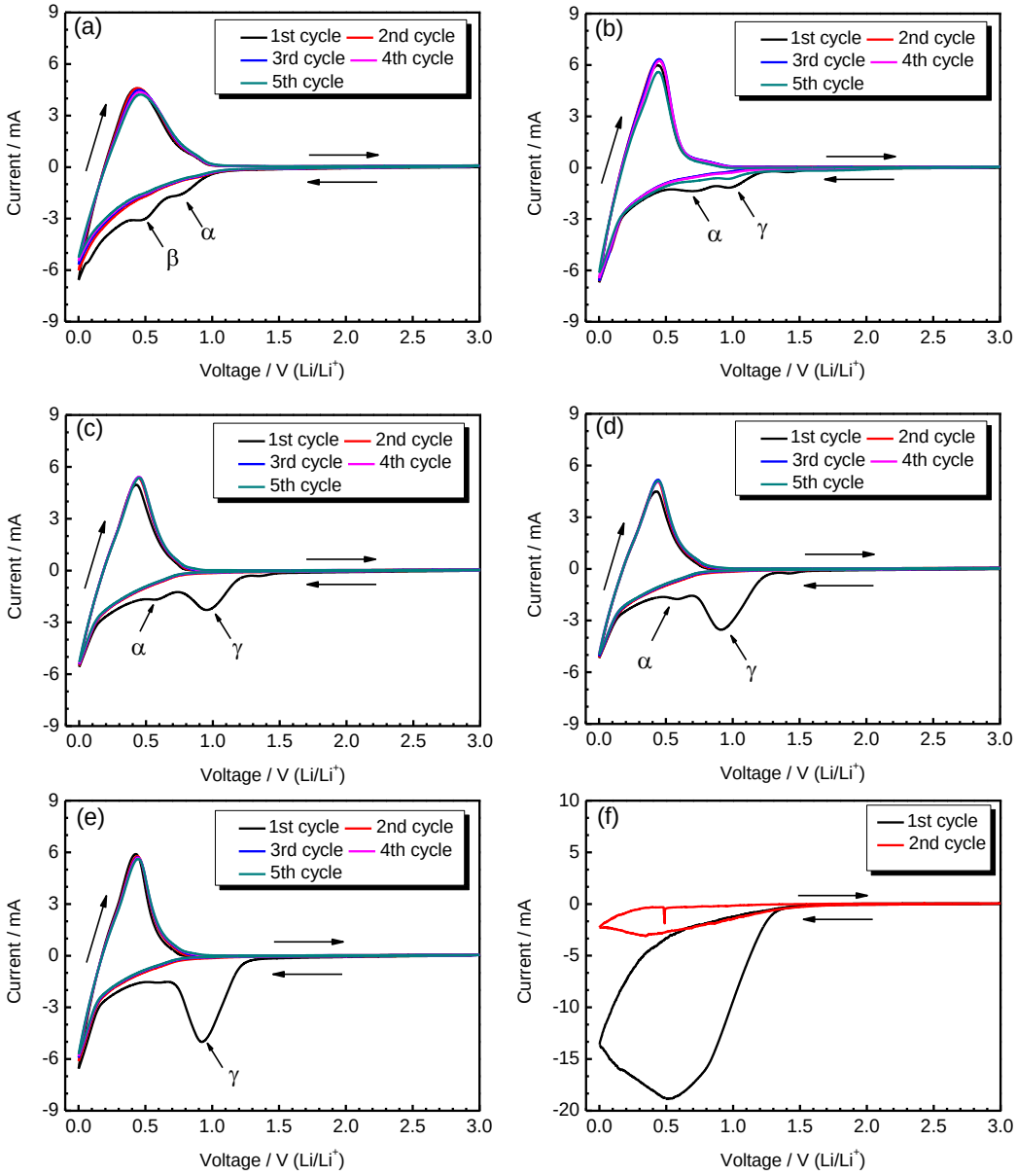

Figure 2. Cyclic voltammetry recorded on graphite electrode in a three-electrode glass cell using the electrolyte of (a) pristine, (b) add 0.5 vol% VEC, (c) add 1.0 vol% VEC, (d) add 3.0 vol% VEC (e) add 5.0 vol% VEC and (f) add 10.0 vol% VEC.

The first step (single electron reduction process):

$$EC + 2e^- + 2Li^+ \rightarrow LiCO_3 + CH_2{=}CH_2$$

The second step (double electrons reduction process):

$$EC + e^- + Li^+ \rightarrow \left[Li^+EC^-\right]$$

$$2\left[Li^+EC^-\right] \rightarrow \left(\text{-}CH_2OCO_2Li\right)_2 + C_2H_4$$

$$2\left[Li^+EC^-\right] \rightarrow \left(\text{-}CH_2\text{-}CH_2\text{-}OCO_2Li\right)_2$$

Therefore, peak α appeared at about 0.8V can be attributed to the formation of Li_2CO_3 by a direct single electron reduction of EC molecule in the electrolyte, peak β located during the potential

range 0.8-0.5 V should be related to the formation of different lithium alkylcarbonates ($ROCO_2Li$) corresponding to the double electrons reduction process of EC. A pair of reduction and oxidation peaks are found around 0.0 and 0.3V, respectively, indicating that the processes of lithium-ion insertion and extraction.

After 0.5 vol% VEC was added into the electrolyte, as shown in Fig. 2(b), it can be seen that peak β disappears and a new reduction peak, γ, is observed in the potential region from 1.3 to 1.0 V, indicating that the formation of lithium alkylcarbonates due to the double electrons reduction process of EC is suppressed. In addition, the current value of peak γ increases with the increase of the content of VEC, as seen in Fig. 2(c) and (d). Just as stated by the above calculations result, VEC has a higher reductive potential than EC, so peak γ could be assigned to the formation of SEI film due to the reductive decomposition of VEC, and the same result was found by Hu et al. [33] in PC-based electrolyte. In subsequent circles, the CV curves of graphite electrode in the VEC-containing electrolyte show good coincidence, which indicates that the cyclic performance of graphite electrode VEC-containing electrolyte is much better than that in the VEC-free electrolyte. It seems that an appropriate content of VEC can improve the reversibility of lithium-ion insertion into and extraction from the graphene layers of the graphite. When the content of VEC is increased to 5.0 vol%, it can be seen form Fig. 2(e) that peak α almost disappear, displaying that the formation of Li_2CO_3 due to the single electron reduction process of EC can also be suppressed. If the superabundant of VEC in electrolyte is introduced, such as 10.0 vol%, only one big reductive peak during the potential range 1.3-0.0 V can be found, as shown in Fig. 2(f), and no oxidation peaks can be observed, indicating that when the single electron reduction process of EC is suppressed completely, it is difficult for lithium ions to intercalate into and deintercalate from the graphite electrode.

Based on the above results, it can be concluded that, for VEC in low content (<5.0 vol%), the formation of $ROCO_2Li$ due to the double electrons reduction process of EC can be suppressed. Generally, the long chain R of $ROCO_2Li$ is expected to interfere badly in both the cohesion and adhesion of SEI film covering on graphite surfaces [34]. On the other hand, too high content of VEC can suppress the formation of Li_2CO_3 due to the single electron reduction process of EC, which is generally regarded as one of the best passivating components for both lithium and graphite electrodes. Thus, when VEC as the film formation additive is added in EC-based electrolyte, the reduction products of EC can also play an important role in the SEI film formation, and choosing an appropriate content of VEC is necessary.

3.3 Charge-discharge test

To further study the effects of the content of VEC on the capacity of graphite electrodes, galvanostatic charge-discharge test was introduced. Fig. 3 presents the charge-discharge curves of the graphite electrode in electrolytes with and without VEC at a constant current of 37 mA g^{-1}. For the cell without any additive, it can be seen from Fig. 3(a), the slowly decreasing potential starts from about 0.8 V, a potential plateau exists in the potential range of 0.8-0.4 V in the first lithium-ion insertion process (corresponding to the first discharge process), so it is obviously ascribed to the reduction of the

electrolyte solvent EC to form SEI film in accordance to CV results, and its discharge capacity is about 20 mAh g^{-1}. The first discharge capacity is 333.6 mAh g^{-1}, while the reversible capacity is 309.9 mAh g^{-1} with a coulombic efficiency of 92.9 %.

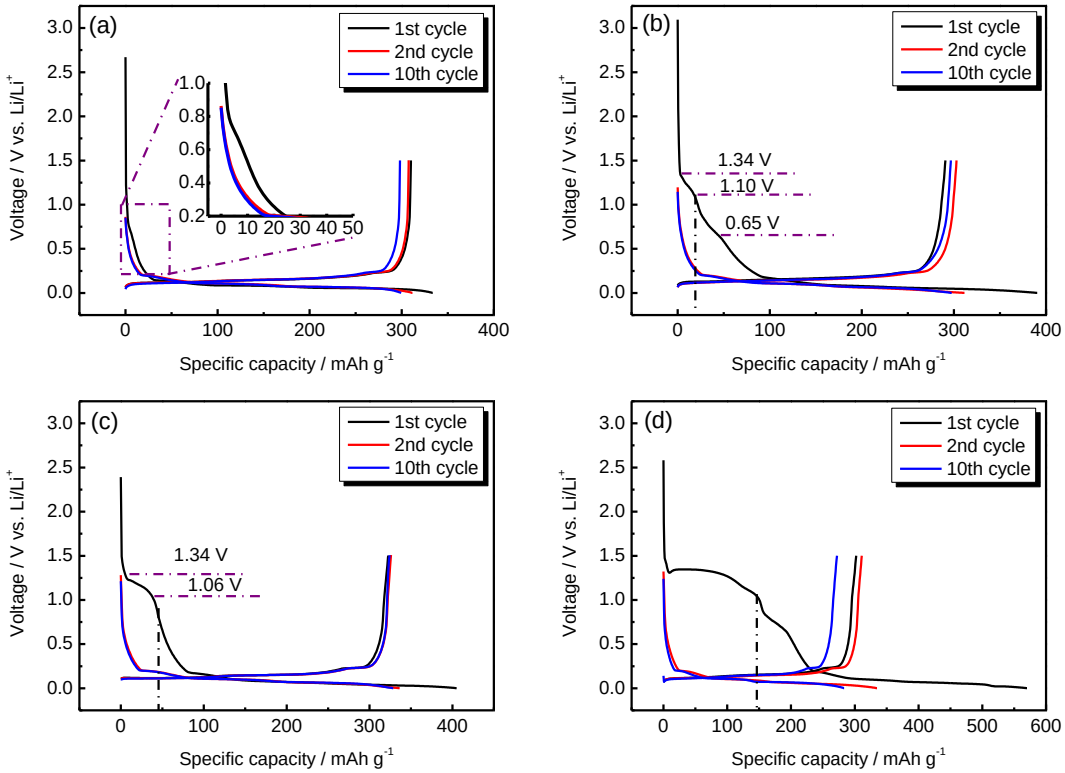

Figure 3. Charge-discharge characteristics of graphite electrode using the electrolyte of (a) pristine, (b) add 0.5 vol% VEC, (c) add 1.0 vol% VEC, (d) add 5.0% VEC.

In contrast, for the cells containing different volume ratio of VEC, the characteristics of the charge-discharge curves are different from the cell with VEC-free electrolyte. For the cell containing 0.5 vol% of VEC, as can be seen from Fig. 3(b), two potential plateaus can be observed during the potential ranges of 1.34-1.10 V and 1.10-0.65 V, which can be attributed to the formation of SEI film due to the decomposition of VEC and EC, respectively, corresponding to our CV results. The first discharge and charge capacities are 390.3 and 290.7 mAh g^{-1}. For the cell with 1.0 vol% of VEC, the first discharge and charge capacities are 405.0 and 323.2 mAh g^{-1} with an irreversible capacity of 81.8 mAh g^{-1} and a coulombic efficiency of 79.8 %. When the content of VEC is further increased to 5.0 vol%, the first discharge and charge capacities are 570.0 and 302.3 mAh g^{-1} with an irreversible capacity of 267.7 mAh g^{-1}, and the coulombic efficiency is only 53.0 %. The decrease of coulombic efficiency for the cells in VEC-containing electrolytes is caused by the big irreversible capacity loss in the first cycle which can be attributed to the formation of SEI film due to the decomposition of VEC on the surface of graphite electrode.

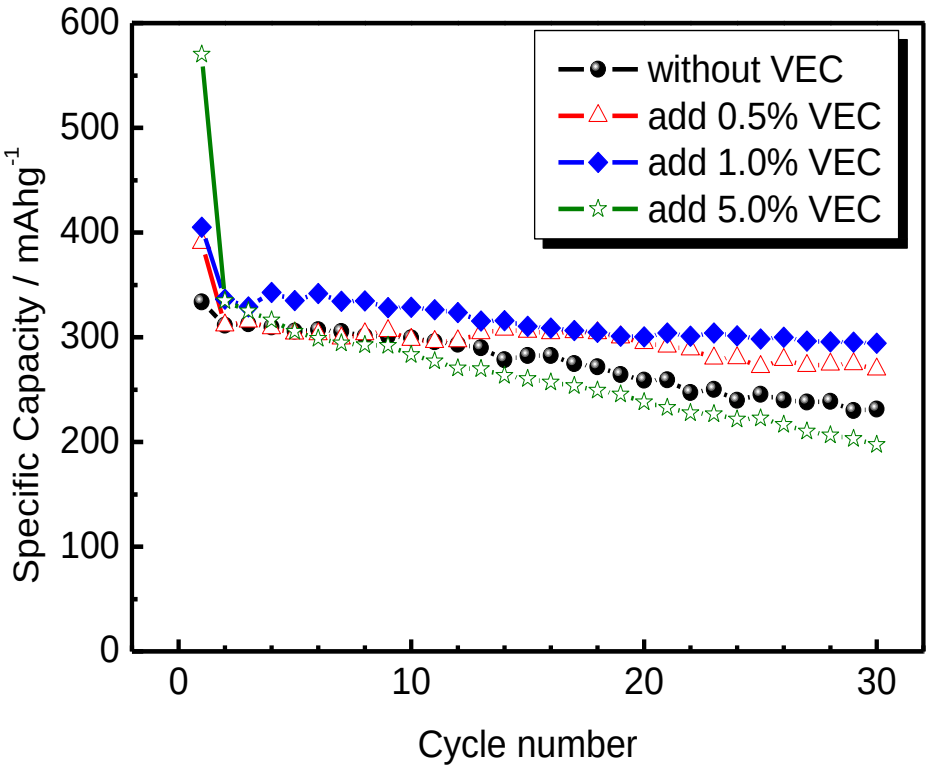

Figure 4. Cycle performance of graphite electrode using 1 mol·L^{-1} $LiPF_6$ in EC: DEC: DMC with or without VEC.

Fig. 4 shows the cycle performance of graphite electrode in VEC-free and VEC-containing electrolytes. The discharge and charge capacity at 1st and 30th cycle and the capacity retention of graphite electrodes in VEC-free and VEC-containing electrolytes are shown in Table 2.

Table 2. A summary of discharge-charge capacity at 1st and 30th cycle and the capacity retention of graphite electrodes in VEC-free and VEC-containing electrolytes.

Electrolyte	1st cycle			30th cycle			Capacity Retention (%)
	Discharge Capacity (mAh g^{-1})	Charge Capacity (mAh g^{-1})	Coulombic Efficiency (%)	Discharge Capacity (mAh g^{-1})	Charge Capacity (mAh g^{-1})	Coulombic Efficiency (%)	
VEC-free	333.6	309.9	92.9	231.5	229.9	99.3	74.2
0.5 % VEC	390.3	290.7	74.5	269.2	268.8	99.8	92.5
1.0% VEC	405.0	323.2	79.8	294.4	294.1	99.9	91.0
5.0 % VEC	570.0	302.0	53.0	197.3	194.3	98.5	64.3

For the cell in VEC-free electrolyte, the 1st and 30th discharge capacity are 333.6 and 231.5 mAh g^{-1}, respectively. For the cells in 0.5 and 1.0 vol% VEC electrolyte, the 30th discharge capacities

are 269.2 and 294.4 mAh g^{-1}, respectively, exhibiting a better cycle performance. However, when the content of VEC is increased to 5.0 vol%, the 30th discharge capacity is only 197.3 mAh g^{-1}, worse than that of the cells in VEC-free electrolyte and in low content of VEC electrolytes (0.5 and 1.0 vol% of VEC), implying that too much additive adding in the electrolyte can not improve the electrochemical property of graphite. Thus, it can be concluded from the charge-discharge result that the electrolyte contains 1.0 vol% of VEC may be an appropriate content.

3.4 FTIR spectroscopy

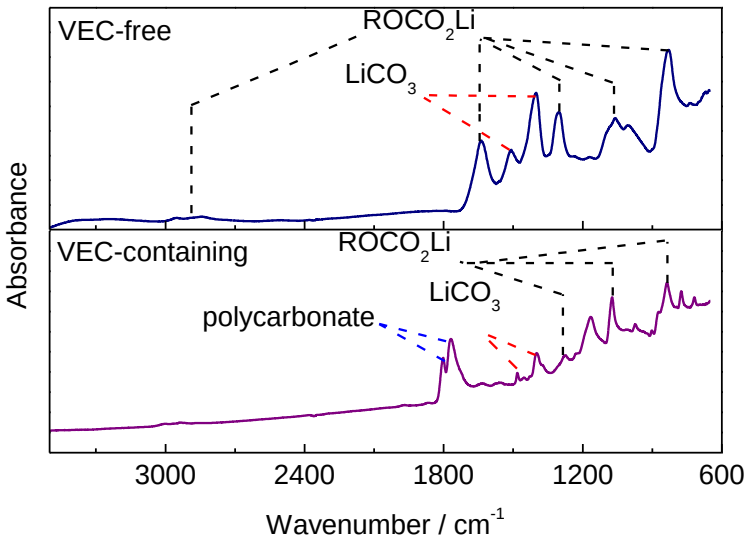

Figure 5. FTIR spectra of the electrode obtained after electrochemical cycles in VEC-free and VEC-containing electrolytes.

Because the composition of the SEI film plays a very significant role in determining the electrochemical performance of lithium-ion battery electrodes, the surface chemistry of the electrodes after cycled in the electrolyte solutions were characterized by using FTIR technique. Fig. 5 shows FTIR spectra of the electrode obtained after electrochemical cycles in VEC-free and VEC-containing electrolytes. For FTIR spectrum of the electrode cycled in VEC-free electrolyte, the pronounced peaks at 2845-2950 cm^{-1} (ν C-H), 1637 cm^{-1} (ν_{as} C=H), 1301 cm^{-1} (ν_{s} C=H), 1060 cm^{-1} (ν C-O) and 829 cm^{-1} (δ OCO_2) are assigned to lithium alkylcarbonates ($ROCO_2Li$) [33,41-43], which are the major reduction products of EC solvent via the double electrons reduction process. The pronounced peaks at around 1508 and 1401 cm^{-1} (ν C-O) belong to the inorganic carbonate, Li_2CO_3, which is mainly formed due to the single electron reduction process of EC. For the spectrum related to the electrode cycled in the VEC-containing electrolyte, the obvious difference is two peaks appeared at around 1802 and 1769 cm^{-1}, which may relate to polycarbonate formed by some polymerization of VEC [24,33]. VEC polymerizes on the graphite surfaces can have a positive effect on the cycling behavior of the electrodes because the SEI film containing VEC polymerizes should be more cohesive and flexible to accommodate the volume changes of graphite electrode during electrochemical cycles, and thus can

provide better passivation than SEI film comprising only Li_2CO_3 and $ROCO_2Li$, the same result is proposed by Aurbach [29] for the effect of VC products on the performance of graphite electrodes.

3.5 Surface morphology

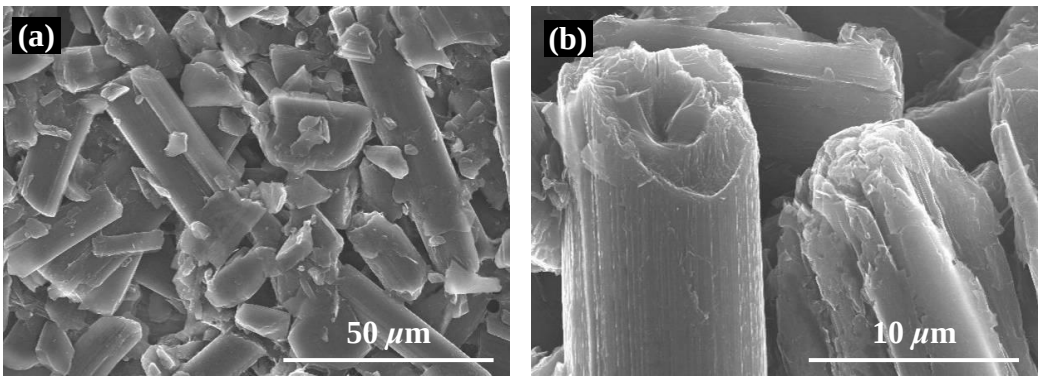

Figure 6. SEM images of graphite electrode before CV cycles.

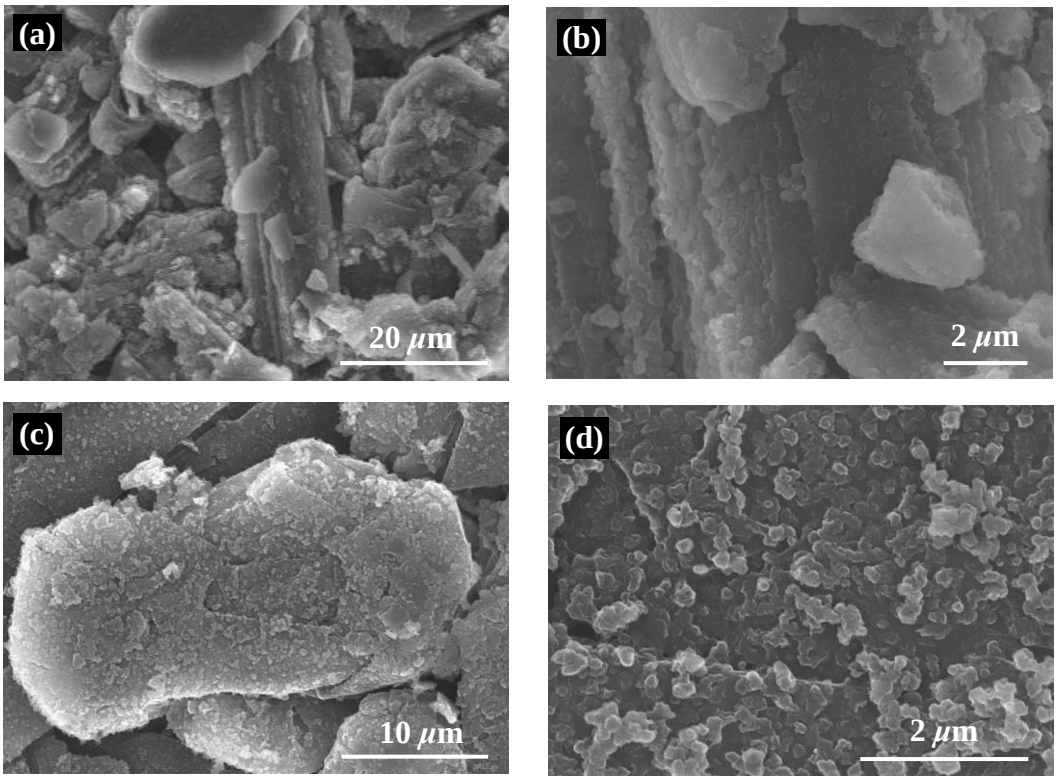

Figure 7. SEM images of graphite electrode after CV cycles in (a), (b) VEC-free electrolyte and (c), (d) VEC-containing electrolyte.

To gain the surface morphology of the graphite electrode before and after cycling in VEC-free and VEC-containing electrolytes, surface observation of the graphite electrode was performed by SEM. Fig. 6 shows the SEM images of the graphite electrode before CV cycles. It can be seen that the graphite materials used in our study show morphology of carbon fibers with a diameter of about 5 μm

and a long of 50 μm, and the surface is smooth before CV cycles. The surface morphologies of the MCF electrodes after ten cycles are shown in Fig. 7. It can be seen from Fig. 7(a) and (b) that the electrode cycled with VEC-free electrolyte has evidence for the formation of an inconsistent rough but dense SEI film, which may be rigid for the volume changes of graphite electrode. Addition of VEC results in an electrode surface which has a complete and uniform VEC-derived SEI film due to the reduction and polymerization of VEC on the graphite electrode.

3.6 EIS characterizations

EIS is one of the most important, highly-resolved electroanalytical techniques that may provide unique information about the nature of electrode processes related to a wide range of time constants [44,45], so EIS measurements were performed on the graphite electrode during the process of the first lithium ion insertion. Fig. 8 depicts the Nyquist plots of the graphite electrodes at various potentials from 3.0 to 0.1 V during the first lithium-ion insertion process in the electrolytes with and without VEC. At open-circuit voltage (OCV~3.0 V), as can be seen in Fig. 8(a)-(b), the impedance spectroscopy of the graphite electrodes are similar to each other, both show a small semicircle in the high-frequency region and a sloping line in the low-frequency region. Because there is no SEI film before the electrochemical cycle, the high frequency semicircle should be assigned to the contact problems that may relate to the contact between the electrolyte and graphite, or graphite and graphite in the electrode bulk, suggested by Holzapfel et al. [46]. The sloping line represents the retardance characteristic of graphite electrode [47]. Along with the decrease of the electrode polarization potential, the Nyquist plots above the potential of 1.5 V are similar with that at the OCV; and no important modification of the impedance spectroscopy can be observed. With the decrease of the electrode potential, the sloping line which is strongly potential-dependent bends toward the real axis and forms a semicircle in the middle-frequency. When the potential drops to 0.8 V, the Nyquist plots for both electrodes are consisted of three parts, essentially two semicircles and one line. According to Aurbach et al. [48-51], the semicircle in the high-frequency region (high-frequency semicircle, abbreviated as HFS) is usually attributed to the SEI film covering on the graphite electrode, the semicircle in the middle-frequency region (middle-frequency semicircle, abbreviated as MFS) is ascribed to charge transfer process at the electrolyte/electrode interface, and the steep sloping line is attributed to solid-state diffusion of the lithium-ion in the graphite matrix. Considering the truth that there has been an initial semicircle in the high-frequency region when the potential is above 1.5 V, here HFS should be related to not only the contact problems but also the migration of lithium-ion migration through SEI film.

According to the experimental results obtained in this work and our previous study of graphite electrode [39], an equivalent circuit, as shown in Fig. 9, is proposed to fit the impedance spectra of the graphite electrode in VEC-containing and VEC-free electrolytes in the first lithium-ion insertion process.

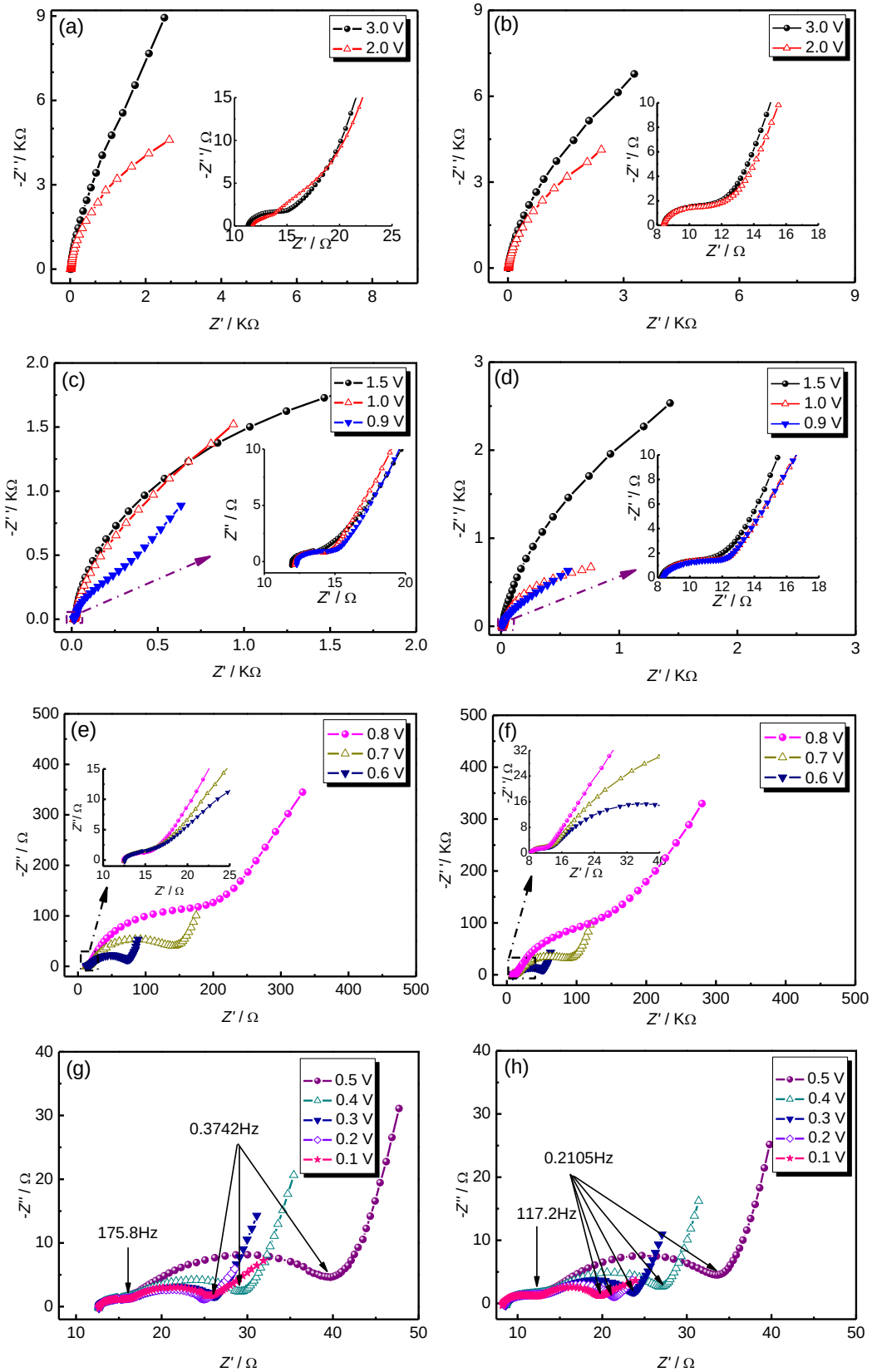

Figure 8. Nyquist plots of the graphite electrode at various potentials from 3.0 to 0.1 V during the first lithium ion insertion process in (a), (c), (e) and (g) VEC-free electrolyte, (b), (d), (f) and (h) VEC-containing electrolyte.

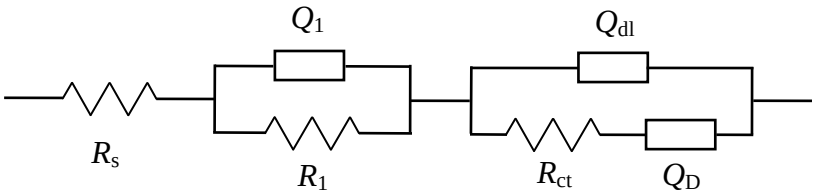

Figure 9. Equivalent circuit proposed for analysis of the graphite electrode during the first lithium-ion insertion process.

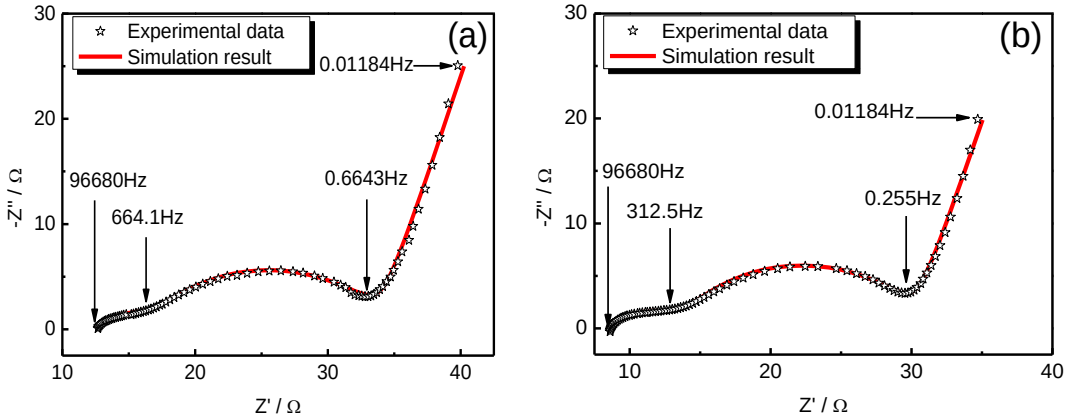

Figure 10. Comparison of EIS experimental data at 0.45 V in the first lithium-ion insertion process with simulation results using the equivalent circuit of Fig. 9.

The resistance-capacitance (*RC*) circuit signifies the semicircle in the Nyquist plots of the EIS. CPE is a constant phase element, and CPE is used instead of capacitance in this study. R_s is the Ohmic resistance; R_1 is the uncompensated resistance, including the resistance of SEI and contact problems. R_{ct} and Q_{dl} represent the charge-transfer resistance and the double-layer capacitance in the middle-frequency region. The low-frequency region, however, cannot be modeled properly by a finite Warburg element. We have chosen, therefore, to replace the finite diffusion by a CPE, that is, Q_D. This approach has been used to characterize the graphite electrode [52] and has allowed us to obtain a good superposition with the experimental data.

Table 3. Equivalent circuit parameters obtained from fitting the experimental impedance spectra at 0.45 V in the first lithium-ion insertion process for the graphite electrode in VEC-free and VEC-containing electrolyte.

parameters	VEC-free		VEC-containing	
	value	error (%)	value	error (%)
R_s	12.5	0.3755	8.39	0.54179
R_{SEI}	4.535	4.6295	5.98	2.9664
Q_{SEI} – n	9.6646×10^{-4}	17.34	6.8322×10^{-4}	11.626
Q_{SEI} – Y_0	0.61323	3.2296	0.57545	2.4117
R_{ct}	17.36	1.423	16.22	1.3561
Q_{dl} – n	4.5051×10^{-3}	2.0191	3.3664×10^{-3}	1.9257
Q_{dl} – Y_0	0.71352	1.1563	0.78758	1.1015
Q_D – n	0.33654	1.1254	0.24862	1.7318
Q_D – Y_0	0.83862	0.54247	0.8419	0.76469

The simulated impedance spectra compared with experimental EIS data for both graphite electrodes in VEC-free and VEC-containing electrolytes at the potential of 0.45 V in the first lithium-ion insertion process are shown in Fig. 10, and the values of the above parameters are listed in Table 3. Some frequencies are added in the experimental Nyquist plots. It can be seen that the proposed model describes the experimental data satisfactorily and the relative standard deviations for most parmeters obtained from fitting the experimental impedance spectra are less than 15 %.

3.7 Variations of R_1 with the electrode potential in the high-frequency region

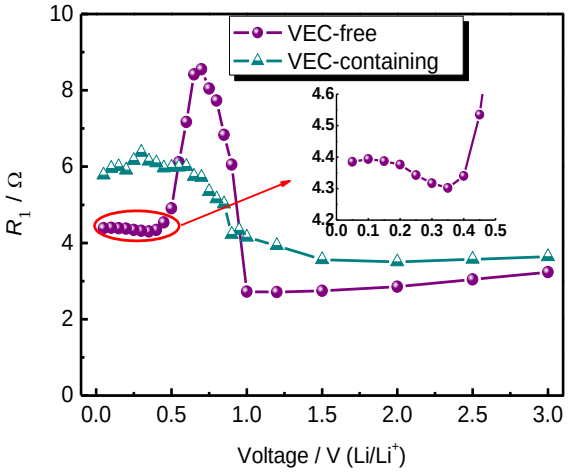

Figure 11. Variation of R_1 with the electrode potential in VEC-free and VEC-containing electrolytes.

Variations of R_1 with electrode potential obtained from fitting the experimental impedance spectra of the graphite electrode in the first lithium insertion process in VEC-free and VEC-containing electrolytes are displayed in Fig. 11. In VEC-free electrolyte, R_1 remains almost invariant with electrode polarization potential decreasing from 3.0 to 1.0 V. Here, R_1 could only be attributed to the contact resistance, as discussed above. On charging from 1.0 to 0.65 V, R_1 increases rapidly, indicating the SEI film begin to form and signifying the increase of the thickness of the SEI film. When the electrode potential is changed from 0.65 to 0.45 V, R_1 decreases rapidly, which may be ascribed to that the reduction products of EC, such as alkyl lithium carbonate, react with the trace amount of water to form a composition with better lithium ion conducting property [17,53], resulting in the SEI film containing more inorganic salts, thus increase the rigidity of SEI film, corresponding to SEM results. With the potential changing from 0.4 to 0.05 V, R_1 increases again, this may be attributed to the processes of the cracking and repairing of the SEI film [54,55]. The SEI film with a rigid structure covering graphite electrode in VEC-free electrolyte can not undergo the volume change of graphite materials upon lithium-ion insertion, leading to the cracking of the SEI film. Subsequently, the reactions of the active mass with electrolyte solution species occur to repair the cracking of the SEI film. The above cracking and repairing of the SEI film lead to an increase in R_1.

However, in VEC-containing electrolyte, on charging from 3.0 to 1.5 V, variations of R_1, which is mainly ascribed to contact resistance, have a similar trend with that in VEC-free electrolyte. With

the decrease of electrode polarization potential from 1.5 to 1.0 V, R_1 increases gradually, reflecting the SEI film due to the reduction and polymerization of VEC begin to form. On further charging from 1.0 to 0.65 V, R_1 increases rapidly, implying the increase of the thickness of the SEI film due to the single electron reduction process of EC to form Li_2CO_3.

In particular, when the potential is changed from 0.65 to 0.05 V, the variation of R_1 is different from that the electrode tested in VEC-free electrolyte. No obvious decrease of R_1 can be found with the potential decreasing from 0.65 to 0.45 V, implying that the reactions between the organic Li salts of the SEI film formed in the VEC-containing electrolyte and the trace amount of H_2O doesn't occur. On further charging from 0.4 to 0.05 V, R_1 does not present an obvious increasing trend, indicating that the SEI film formed in the VEC-containing electrolyte should be more flexible to accommodate with the volume changes, and the cracking and repairing of the SEI film are avoided, as a result contributes to the cycle performance of electrode, which is consistent with the above CV and charge-discharge results.

3.8 Variation of R_{ct} with electrode potential in the middle-frequency region

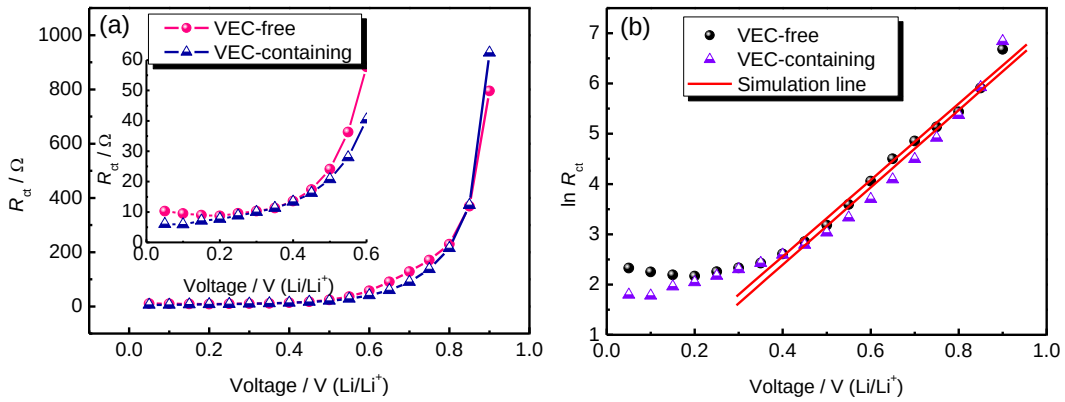

Figure 12. Variations of R_{ct} and lnR_{ct} with the electrode potential in VEC-free and VEC-containing electrolytes.

Fig. 12 reflect the dependence of R_{ct} and the logarithmic of R_{ct} on the electrode potential in VEC-free and VEC-containing electrolytes. As can be seen from Fig. 12(a), for both electrolytes, R_{ct} decreases with the decrease of electrode polarization potential from 0.9 to 0.5 V during the first lithium ion insertion process and R_{ct} essentially has a small value below the potential of 0.4 V. However, R_{ct} is smaller when VEC is present in the electrolyte solution, indicating that it is easier for lithium ions to insert into and extract from the graphite electrode in VEC-containing electrolyte.

According to our previous study [39], R_{ct} can be written as:

$$R_{ct} = \frac{RT}{n_e^2 F^2 c_{max} k_0 \left(M_{Li^+}\right)^{(1-\alpha_f)}} \exp\left[\frac{-\alpha_f F\left(E-E_0\right)}{RT}\right] \quad (5)$$

where R and T represent the thermodynamic constant and temperature, respectively, n_e is the number of electrons exchanged on the processes of lithium-ion insertion and extraction, F is the

Faraday constant, i_0 is the exchange current density, c_{max} (mol cm^{-3}) is the maximum concentration of lithium ion in graphite electrode, M_{Li^+} is the concentration of lithium ion in the electrolyte near the electrode, k_0 represents the standard reaction speed constant, E and E_0 define the electrode's real and standard potentials, and α_f is representing symmetry factor for the electrochemical reaction.

Make Equation (5) to linear equation by logarithm, we can get the relation between the lnR_{ct} and the potential:

$$\ln R_{ct} = \ln \frac{RT}{n_e^2 F^2 c_{max} k_0 \left(M_{Li^+}\right)^{(1-\alpha_f)}} - \frac{\alpha F\left(E - E_0\right)}{RT} \quad (6)$$

It can be seen from Equation (6), that R_{ct} decreases in an exponential manner with the decreasing of potential when the insertion level $x \rightarrow 0$, which coincides with our simulation data, just as shown in Fig. 12(b). lnR_{ct} is linear with the electrode potentials in the potential region from 0.9-0.4 V in the first lithium ion insertion process in both VEC-free and VEC-containing electrolytes. Also, the symmetry factor, α_f, can be calculated from the slope of the simulation line. The calculated values of α_f in VEC-free and VEC-containing electrolytes are 0.1963 and 0.2105, respectively, implying that the reversibility of charge transfer reaction during the lithium ion insertion and extraction processes is improved in VEC-containing electrolyte.

4 CONCLUSIONS

In this work, the influence of the content of VEC as SEI film forming additive in EC-based electrolyte on the formation mechanisms of SEI film at the surface of graphite electrode is investigated by CV and charge-discharge analysis combined with FTIR SEM and EIS technologies. The main conclusions can be summarized as follows:

(*i*) In the case of electrolyte containing low content of VEC, the formation of $ROCO_2Li$ due to the double electrons reduction process of EC can be suppressed, thus improved the electrochemical performance of graphite electrodes.

(*ii*) In the case of electrolyte containing high content of VEC, the formation of Li_2CO_3 due to the single electron reduction process of EC can be also suppressed, that may take an adverse effect on the cycle performance of graphite electrodes.

(*iii*) According to FTIR, SEM and EIS results, the major components of the SEI film covering the graphite electrode in VEC-containing electrolyte are VEC polymerizes, Li_2CO_3 and $ROCO_2Li$. The VEC-derived SEI film, consisting of a polymeric species, are capable of resisting the attack of the trace amount of the impurities such as H_2O in the electrolyte, and by providing better passivation than the SEI film only comprising Li_2CO_3 and $ROCO_2Li$. Hence, the SEI film covering graphite electrodes in VEC-containing electrolyte can be more stable during the lithium ions insertion, and be flexible to accommodate the volume changes of graphite material, resulting in a better reversibility of lithium ions insertion and extraction.

The specific data herein are of interest, and the general conclusions may help development of the application of VEC for enhanced lithium-ion battery.

ACKNOWLEDEMENTS
This work was supported by "the Fundamental Research Funds for the Central Universities" (2010LKHX03, 2012LWB23) and major State Basic Research Development Program of China (2009CB220102).

References

1. J.-M. Tarascon, M. Armand, *Nature* 414 (2001) 359.
2. M. Armand, J.-M. Tarascon, *Nature* 451 (2008) 652.
3. S. S. Zhang, *J. Power Sources* 162 (2006) 1379.
4. P. Verma, P. Maire, P. Novák, *Electrochim. Acta* 55 (2010) 6332.
5. K. Xu, *Chem. Rev.* 104 (2004) 4303.
6. H. Buqa, A. Würsig, J. Vetter, M. E. Spahr, F. Krumeich, P. Novák, *J. Power Sources* 153 (2006) 385.
7. S. Tsubouchi, Y. Domi, T. Doi, M. Ochida, H. Nakagawa, T. Yamanaka, T. Abe, Z. Ogumi, *J. Electrochem. Soc.* 159 (2012) A1786.
8. H. Bryngelsson, M. Stjerndahl, T. Gustafsson, K. Edström, *J. Power Sources* 174 (2007) 970.
9. E. Peled, D. B. Tow, A. Merson, A. Gladkich, L. Burstein, D. Golodnitsky, *J. Power Sources* 97-98 (2001) 52.
10. S.-P. Kim, A. C. T. van Duin, V. B. Shenoy, *J. Power Sources* 196 (2011) 8590.
11. K. Edström, M. Herstedt, D. P. Abraham, *J. Power Sources* 153 (2006) 380.
12. Y. Ein-Eli, S. R. Thomas, V. R. Koch, *J. Electrochem. Soc.* 144 (1997) 1159.
13. J.-S. Shina, C.-H. Hana, U.-H. Jung, *J. Power Sources* 109 (2002) 47.
14. Y.-K. Choi, K. Chung, W.-S. Kim, Y.-E. Sung, S.-M. Park, *J. Power Sources* 104 (2002) 132.
15. K. Chung, J.-D. Lee, E.-J. Kim, W.-S. Kim, J.-H. Cho, Y-K Choi, *Microchem. J.* 75 (2003) 71.
16. H. Zheng, Y. Fu, H. Zhang, T. Abe, Z. Ogumi, *Electrochem. Solid-State Lett.* 9 (2006) A115.
17. Q.-C. Zhuang, J. Li, L.-L. Tian, *J. Power Sources* 222 (2013) 177.
18. Y. An, P. Zuo, X. Cheng, L. Liao, G. Yin, *Electrochim. Acta* 56 (2011) 4841.
19. G. H. Wrodnigg, J. O. Besenhard, M. Winter, *J. Electrochem. Soc.* 146 (1999) 470.
20. G. H. Wrodnigg, T. M. Wrodnigg, J. r. O. Besenhard, M. Winter, *Electrochem. Commun.* 1 (1999) 148.
21. W. Yao, Z. Zhang, J. Gao, J. Li, J. Xu, Z. Wang, Y. Yang, *Energy Environ. Sci.* 2 (2009) 1102.
22. B. Li, M. Xu, T. Li, W. Li, S. Hu, *Electrochem. Commun.* 17 (2012) 92.
23. C.-C. Chang, S.-H. Hsu, Y.-F. Jung, C.-H. Yang, *J. Power Sources* 196 (2011) 9605.
24. V. Etacheri, O. Haik, Y. Gofer, G. Roberts, I. Stefan, R. Fasching, D. Aurbach, *Langmuir* 28 (2012) 965.
25. S. Dalavi, P. Guduru, B. L. Lucht, *J. Electrochem. Soc.* 159 (2012) A642.
26. N.-S. Choi, K. H. Yew, K. Y. Lee, M. Sung, H. Kim, S.-S. Kim, *J. Power Sources* 161 (2006) 1254.
27. R. Elazari, G. Salitra, G. Gershinsky, A. Garsuch, A. Panchenko, D. Aurbach, *J. Electrochem. Soc.* 159 (2012) A1440.
28. L. Chen, K. Wang, X. Xie, J. Xie, *J. Power Sources* 174 (2007) 538.
29. D. Aurbach, K. Gamolsky, B. Markovsky, Y. Gofer, M. Schmidt, U. Heider, *Electrochim. Acta* 47 (2002) 1423.
30. L. El Ouatani, R. Dedryvère, C. Siret, P. Biensan, S. Reynaud, P. Iratçabal, D. Gonbeau, *J. Electrochem. Soc.* 156 (2009) A103.
31. H.-C. Wu, C.-Y. Su, D.-T. Shieh, M.-H. Yang, N.-L. Wu, *Electrochem. Solid-State Lett.* 9 (2006) A537.
32. K. Tasaki, K. Kanda, T. Kobayashi, S. Nakamura, M. Ue, *J. Electrochem. Soc.* 153 (2006) A2192.

33. Y. Hu, W. Kong, H. Li, X. Huang, L. Chen, *Electrochem. Commun.* 6 (2004) 126.
34. Y. Hu, W. Kong, Z. Wang, H. Li, X. Huang, L. Chen, *Electrochem. Solid-State Lett.* 7 (2004) A442.
35. T.-H. Nam, E.-G. Shim, J.-G. Kim, H.-S. Kim, S.-I. Moon, *J. Electrochem. Soc.* 154 (2007) A957.
36. Y. Fu, C. Chen, C. Qiu, X. Ma, *J. Appl. Electrochem.* 39 (2009) 2597.
37. R. Chen, F. Wu, L. Li, Y. Guan, X. Qiu, S. Chen, Y. Li, S. Wu, *J. Power Sources* 172 (2007) 395.
38. Y. Matsuo, K. Fumita, T. Fukutsuka, Y. Sugie, H. Koyama, K. Inoue, *J. Power Sources* 119-121 (2003) 373.
39. S.-D. Xu, Q.-C. Zhuang, L.-L. Tian, Y.-P. Qin, L. Fang, S.-G. Sun, *J. Phys. Chem. C* 115 (2011) 9210.
40. A. Naji, J. Ghanbaja, P. Willmann, B. Humbert, D. Billaud, *J. Power Sources* 62 (1996) 141.
41. A. Naji, J. Ghanbaja, B. Humbert, P. Willmann, D. Billaud, *J. Power Sources* 63 (1996) 33.
42. A. Zaban, D. Aurbach, *J. Power Sources* 54 (2005) 289.
43. D. Aurbach, *J. Electrochem. Soc.* 141 (1994) L1.
44. X.-Y. Qiu, Q.-C. Zhuang, Q.-Q. Zhang, R. Cao, P.-Z. Ying, Y.-H. Qiang, S.-G. Sun, *Phys. Chem. Chem. Phys.* 14 (2012) 2617.
45. Q.-C. Zhuang, T. Wei, L.-L. Du, Y.-L. Cui, L. Fang, S.-G. Sun, *J. Phys. Chem. C* 114 (2010) 8614.
46. M. Holzapfel, A. Martinent, F. Alloin, B. Le Gorrec, R. Yazami, C. Montella, *J. Electroanal. Chem.* 546 (2003) 41.
47. Y. C. Chang, H. J. Sohn, *J. Electrochem. Soc.* 147 (2000) 50.
48. M. D. Levi, D. Aurbach, *J. Phys. Chem. B* 101 (1997) 4630.
49. D. Aurbach, M. D. Levi, E. Levi, H. Teller, B. Markovsky, G. Salitra, U. Heider, L. Heider, *J. Electrochem. Soc.* 145 (1998) 3024.
50. B. Markovsky, M. D. Levi, D. Aurbach, *Electrochim. Acta* 43 (1998) 2287.
51. D. Aurbach, *J. Power Sources* 89 (2000) 206.
52. S. Zhang, P. Shi, *Electrochim. Acta* 49 (2004) 1475.
53. D. Aurbach, Y. Ein-Eli, B. Markovsky, A. Zaban, S. Luski, Y. Carmeli, H. Yamin, *J. Electrochem. Soc.* 142 (1995) 2882.
54. C. Wang, I. Kakwan, A. J. Appleby, F. E. Little, *J. Electroanal. Chem.* 489 (2000) 55.
55. C. Wang, A. J. Appleby, F. E. Little, *J. Electroanal. Chem.* 497 (2001) 33.